R-107
NRL

Electron Microscope Method for Measuring Diffraction Grating Groove Geometry

W. A. Anderson, G. L. Griffin, C. F. Mooney, R. S. Wiley

ABSTRACT

This paper reports an electron microscope method developed for measuring grating groove depths. The method was used recently for a set of test gratings with 1280 grooves/mm that were blazed in the vacuum ultraviolet. The efficiency of some of these gratings was later measured as a function of wavelength using spectrographic facilities at the Naval Research Laboratory. The correspondence between the blaze wavelengths measured for these gratings by the electron microscope method and by the wavelength of peak performance efficiency is reported. All of the gratings studied were ruled in gold with a groove step height near 500 Angstroms.

The authors are with Bausch & Lomb Incorporated.

This work was supported in part by the E. O. Hulburt Center for Space Research of the U. S. Naval Research Laboratories with a grant from the National Aeronautic and Space Administration.

Introduction

Two approaches have been used by electron microscopists for examining the profile contour of grooves. First, the stereo-photogrammetric approach pioneered by Heidenreich and Matheson[1] would be essential for three dimensional objects of arbitrary topography and there is much current activity based on this approach. Second, Seeliger[2] has used oblique shadowing past an oriented glass fiber to exhibit groove profiles. This fiber-shadow approach is limited in practical application to regular surfaces because profile information is provided only at a special set of points (the shadow demarcation line) across the face of the object.

In both approaches, a specimen-replica that is transparent to electrons must be used in the microscope. Despite their fragility, these specimens need somehow to store the depth detail of the original object until electron micrographs are taken.

Specimen preparation methods for the stereo-micrograph approach are believed to be inherently subject to losses of depth information because the information is stored only by the fragile contours of the specimen. The fiber-shadow method described here fixes the depth information in the shadow-line while the specimen is still massive.

Groove Depth Information from Electron Microscope Method

Fig. 1 is an electron micrograph of grating grooves in plan view. The groove profile has been displayed as the shadow cast by evaporating a heavy metal obliquely past an asbestos fiber. This fiber appears here as a straight black rod lying across the terminal groove and adjacent unruled area. The white band in Fig. 1 is unmetallized area in the shade of the obstacle. The shadow boundary line is a projection onto the grating profile of the top edge of the fiber. The grating elevation therefore appears as an overlay on this plan view. Where the shadow boundary is closest to the fiber, the specimen replica of the grating has a ridge line. Where the boundary is more remote, the replica has a valley. It is evident that the aluminum in which these grooves were ruled has been smoothed by the burnishing diamond. It is also evident that the groove detail and consequently, the shadow edge detail is influenced by the residual film roughness. Another point to note is that the steep side of the terminal groove can be clearly seen whereas it has been pushed almost out of sight in the preceding groove.

An electron micrograph of a .83 micron sphere also appears in Fig. 1. The ratio of the shadow width to its length is, with some correction, used to measure the tangent of the angle of oblique shadowing. This angle is needed to calculate the anamorphic magnification factor of the projection.

Electron Microscopy Procedure

Fig. 2 depicts the sequence of operations used in making the electron microscope specimens. The grating is coated with about a micron of Al, then with a flash of Mg that prevents the development of a persistent Al_2O_3 film on this surface. This was a procedure reported by Hass and McFarland[4] in their preparation of aluminum oxide replicas. A section of this composite film is lifted from the grating using tape by stripping parallel to the grooves. Asbestos fibers are sprinkled randomly onto the oxide-covered aluminum surface now exposed, and the film is returned to the stage of the vacuum coater for oblique platinum shadowing and for carbon deposition normal to the surface. The platinum is distilled from a pellet of compressed carbon and platinum; the carbon is sublimed from the interface of a pointed carbon rod held against a flattened carbon rod by a spring.

The point of this technique sequence is to fix the groove depth information by shadowing the preliminary specimen while it is thick and robust. The thick Al is subsequently dissolved in dilute HCl leaving the thin carbon replica and the platinum-carbon shadow film as the only residual films through which electrons must pass in the microscope. After shadowing, specimens need not retain their depth contour accurately; the original profile has been stored on the plan view by the shadow line.

Electron microscope photographs similar to Fig. 1 are taken on 35 mm film and developed for measurement.

Measurement of Groove Depth and Shape

Fig. 3 illustrates three geometric factors that enter the formula for groove depth calculations. These factors are: 1) The scale factor, given here by the known distance between grating grooves, 2) the shadow slope, given here by the ratio of the ball shadow width to its shadow length, and 3) the groove slope, given here by certain angular relationships of the fiber and of its shadow to the direction of the grooves.

C in Fig. 3 is the angle between a line perpendicular to the groove direction and a line that is parallel to the fiber as projected onto the average plane of the grating. B is the angle between this projected fiber direction onto the average plane of the grating and the direction of the shadow demarcation line on the groove slope as it appears in plan view.

Measurement of the ball shadow and of the angular relationships are made directly from the 35 mm film micrograph with the help of a 10-inch contour projector equipped with a protractor ring screen.

Fig. 3 is appropriate for calculating the groove depth h. Grating analysis, however, needs the perpendicular distance between tangent planes to corresponding areas of adjacent grooves. For this, a cosine factor must be included and the value of g then used is the grating groove separation rather than the groove width. For the gratings discussed in this report, the grooves are so shallow relative to their width that this correction is hardly significant.

Recognized Limitations of Method

Because the electron microscope method provides the groove profile only at one section through the groove, local groove surface roughness makes the grooves appear to have various and irregular shapes. In many cases, this is the most important limit on measurement precision.

The precision for gratings whose grooves are smooth, flat, and parallel is limited by the latex ball shadow measurements. The elliptical shadow occurs on a sloping background that regularly falls away into an adjacent groove. Measurement requires extrapolated settings because one end of the shadow is under the ball and the other is diffused.

Additional phenomena that may limit the reliability of the method are:

1. Stretching of the replica while lifting it by tape prior to shadowing.

2. Misalignment of the shadow vapor direction with groove direction.

In order to learn how closely the geometric measurements obtained by the electron microscope method agreed with spectral efficiency measurements, fifty similar (10 mm ruled width with 1280 grooves/mm) test rulings were made and forty-one of these were examined both with the electron microscope method and with grating efficiency test facilities. The spectroscopic equipment used is located at the Naval Research Laboratory. It was developed by W.R. Hunter with the assistance of D.W. Angel, and it was operated under their supervision. Information from this study about the accuracy of the electron microscope method is given below.

Groove Geometry and Spectral Performance

The grating blaze wavelengths expected geometrically and measured spectroscopically of twenty-five of the forty-one experimental gratings are listed in Table I. Test rulings prior to number NRL 20 as well as numbers 27, 30, and 32 have been excluded because of their generally rough surface texture. Several others have been excluded because they have an extremely broad blaze or because the spectroscopic measurements did not include the blaze peak.

The agreement shown by Table I between these two types of measurements is better than had been expected in view of experimental uncertainties.

Two gratings have been selected from the forty-one studied for inclusion in this report in order to illustrate a particularly excellent grating (NRL 42) that is included in Table I and a grating (NRL 34) that could not be included because no clear blaze peak was observed spectroscopically.

Fig. 4 is a pair of electron micrographs from ruling 42. Micrograph A shows the grooves to be flat, smooth, and parallel. This grating approaches the ideal case more closely than any of the other twenty-four gratings in Table I. Micrograph B in Fig. 4 shows unruled area on the same blank.

Fig. 5 is a schematic drawing of the groove profile showing the calculated step height and the groove slope (blaze) angle of the grating. The perpendicular distance between the tangent plane to adjacent groove faces was measured from the electron micrograph to be 450 ± 65Å. This step height corresponds to a groove face angle or blaze angle of $3.3^{\circ} \pm .5^{\circ}$.

Fig. 6 is the measured efficiency curve of test grating NRL 42. The peak diffraction efficiency of the first spectral order was actually higher than the highest reflectance value obtained at the same wavelength for unruled gold films, but the possibility of comparable amounts of measurement error has made it advisable to normalize the ordinate values on an arbitrary scale. The data were first, however, corrected for wavelength dependence by dividing the measured reflectance at different wavelengths by the reflectance of gold at the corresponding

wavelengths. The standardizing reflectance values used to adjust the wavelength dependence were taken from work reported by Canfield, Hass, and Hunter.[5] The abscissa is linear with respect to wavenumber to avoid improper emphasis of the longer wavelength spectral region and to exhibit any symmetry of the diffracted distribution. The zero order is shown as never exceeding .02 on the same scale.

Spectral diffraction measurements were made with light incident at 5° to the grating surface normal. The spectrum orders measured were on the opposite side of the grating normal from the incident radiation. The grating blaze angle θ of flat groove faces can be calculated from an expression of the grating equation in terms of the incidence direction A relative to the groove face normal. For the first order spectrum, this equation is:

$$\sin \theta = \lambda_B G/2 \cos A,$$

where λ_B is the wavelength diffracted most efficiently (blazed), where $A = \theta + 5^{\circ}$, and where G is the groove frequency. λ_B was near 840 Å and 1/G was 7801 Å, whence $\theta \approx 3.12^{\circ}$. In principle, θ is found by successive approximations that improve the value of $A \approx 8.15^{\circ}$; in practice, cos A is not sensitive to the values of θ when A is this small. The uncertainties of the spectroscopic measurement include the choice of a curve for correcting the wavelength dependence of the reflectance of the particular gold film used. For example, the composite curve of the highest gold reflectance that was measured

shifts the apparent blaze wavelength of NRL 42 to 950 Å and produces a calculated $\theta' \approx 3.52°$.

Fig. 7 contains the electron micrographs of ruled and unruled parts of test grating NRL 34. The groove faces appear to be convexly curved. Fig. 8 is a graph of the diffraction efficiency relative to the gold reflectance reported by Canfield, Hass, and Hunter[5]. Test grating NRL 34 is almost uniformly efficient over an extended range of wavelengths. It is not appropriate to inquire at what wavelength such a grating is blazed.

The authors are grateful for the use of spectroscopic efficiency measurement facilities at the Naval Research Laboratories and to W. R. Hunter and D. W. Angel for supervising its use. The authors also thank R. Tousey and J. D. Purcell of the Naval Research Laboratories and D. Richardson, and E. G. Loewen of Bausch & Lomb for support and advice in performing this work. The test gratings were ruled by J. Beckenbach.

Table I. Grating blaze wavelengths in Ångströms geometrically predicted from the electron microscope method and directly measured from spectral diffraction efficiency.

Test Ruling	Doubled Step Height	First Order Peak
20	1130	950
21	1230	1080
22	1100	840
23	1200	1040
24	840	760
25	840	700-930
26	900	920
28	810	860
31	810	780
35	890	850
37	1000	950
38	940	950
39	780	850
40	1000	830-1030
41	1080	950
42	900	950
43	840	850
44	780	880
45	940	830-950
46	800	900
47	900	850
48	840	800-950
49	860	800-1000
51	1040	940
52	1080	1030

REFERENCES

1. R. Heidenreich and L. Matheson, J. Appl. Phys. 15, 423 (1944).

2. R. Seeliger, Z. Metallkunde 39, 170-2 (1948).

3. H. D. Babcock, J.O.S.A. 34, 1 (1944).

4. G. Hass and M. E. McFarland, J. Appl. Phys. 21, 435 (1950).

5. Canfield, Hass, and Hunter, J. Phys. 25, pp. 124-129 (1964).

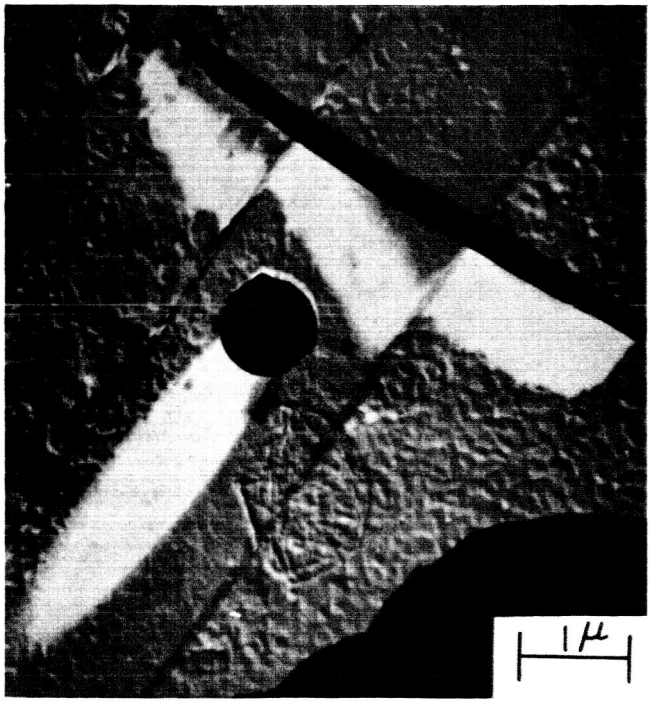

Fig. 1. Electron micrograph showing the profile of the terminal grooves of a diffraction grating in the shadow cast by an asbestos fiber. The 0.83 micron latex sphere shows the angle at which the shadowing vapor was incident.

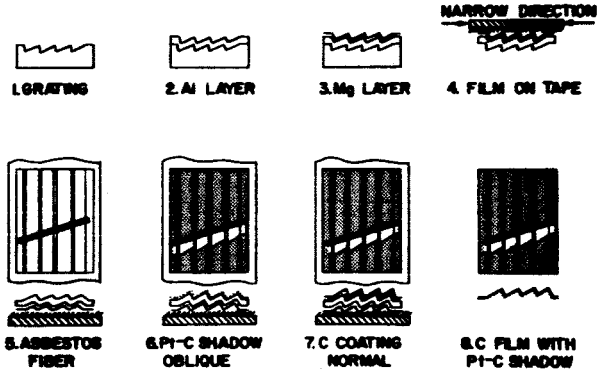

Fig. 2. Sequence of shadowing technique steps to fix groove depth information prior to electron microscopy.

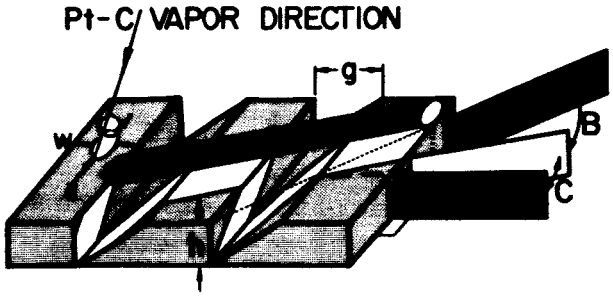

$$h = g(\ell/w)\ [\tan(B+C) - \tan C]$$

Fig. 3. Geometric relationships for analyzing the shadow of a straight edge in a simple groove.

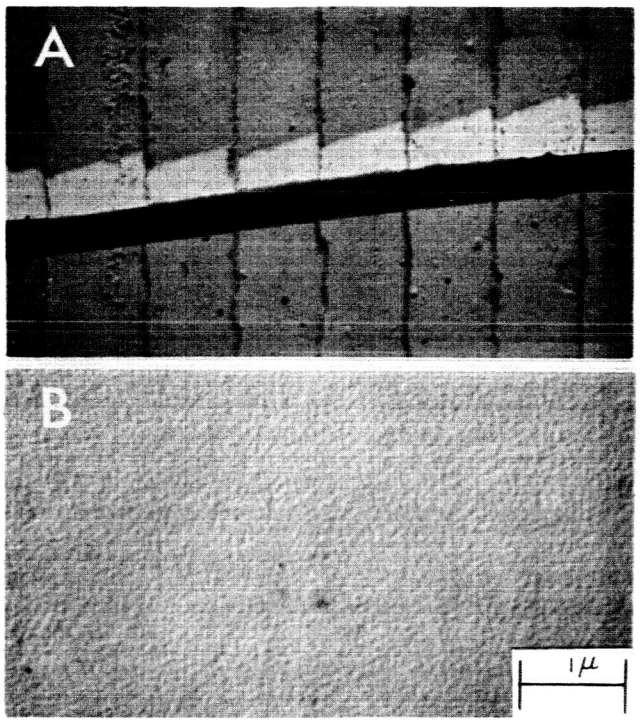

Fig. 4. Electron micrograph of grating NRL 42, A) ruled grooves, B) unburnished film.

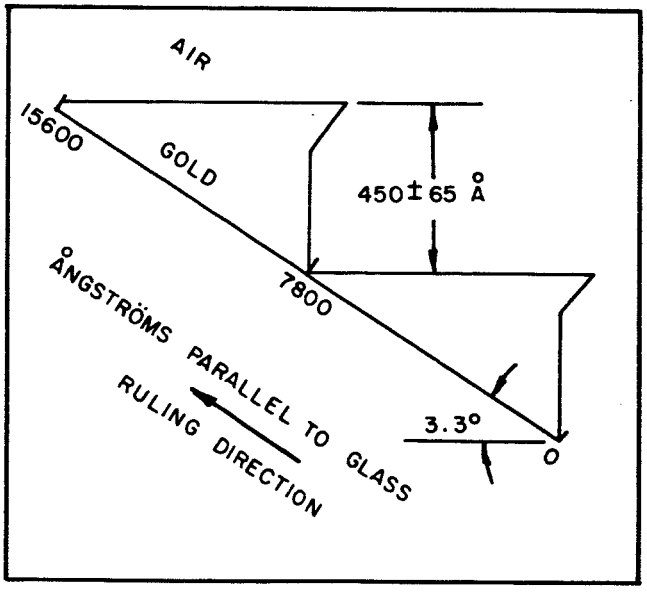

Fig. 5. Schematic form of grating profile NRL 42.

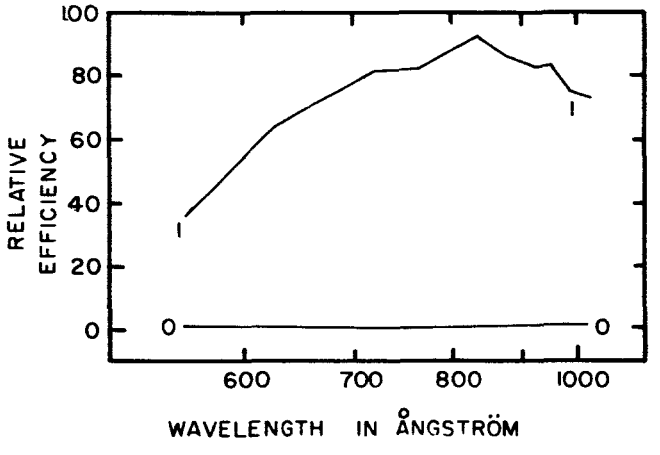

Fig. 6. Relative diffraction efficiency of test grating NRL 42. The ordinate scale is arbitrary, and corrected for the dispersion of reflectance by gold.

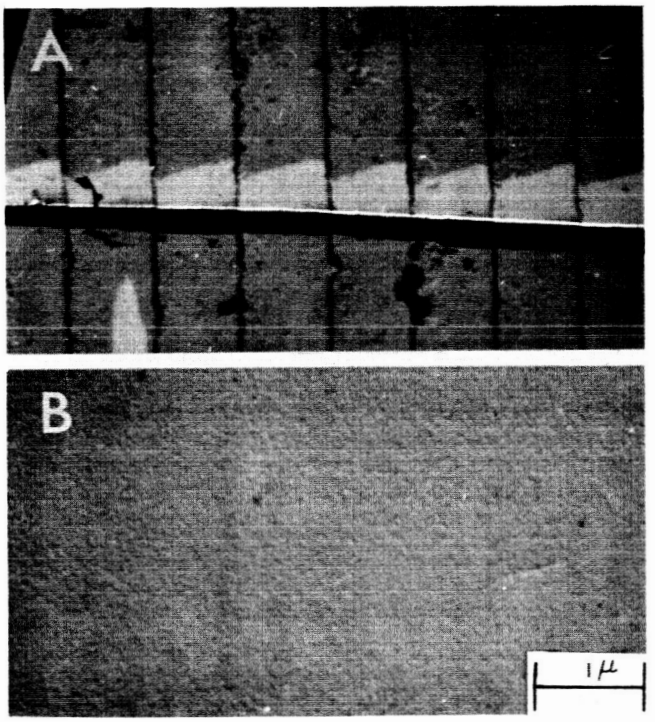

Fig. 7. Electron micrographs of grating NRL 34, A) ruled grooves, B) unburnished film.

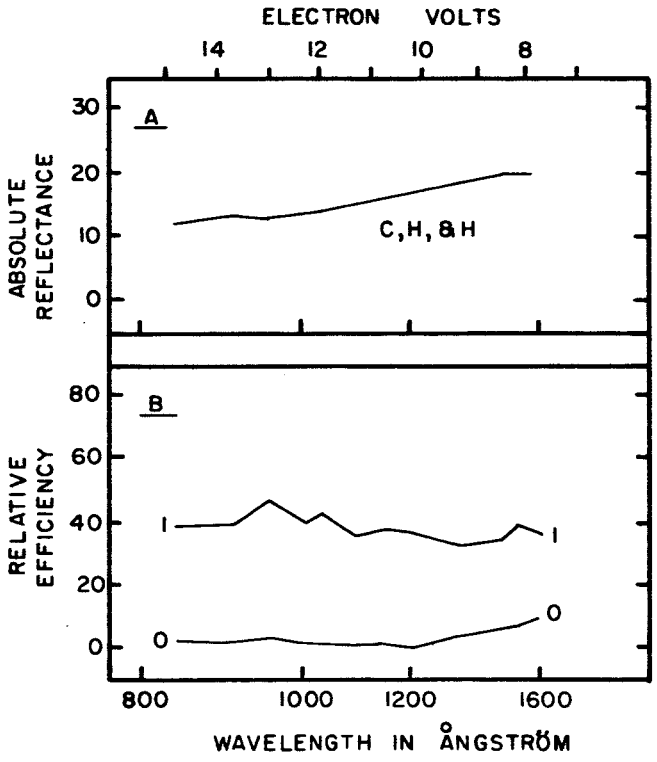

Fig. 8. Relative diffraction efficiency in several orders of test ruling NRL 34 are plotted in frame B. The ordinate values of B were obtained by dividing measured efficiencies by the corresponding spectral reflectances reported in reference 3. These reflectances are plotted on an absolute scale in frame A.